Level-set simulation for the strain-driven sharpening of the island-size distribution during submonolayer heteroepitaxial growth

C. Ratsch,[1,2] J. DeVita,[1] and P. Smereka[3]
[1]*Department of Mathematics, UCLA, Los Angeles, California 90095, USA*
[2]*Institute for Pure and Applied Mathematics, UCLA, Los Angeles, California 90095, USA*
[3]*Department of Mathematics, University of Michigan, Ann Arbor, Michigan 48109, USA*
(Received 14 February 2009; revised manuscript received 1 September 2009; published 8 October 2009)

We use an island dynamics model for heteroepitaxial growth to study the narrowing and sharpening of the island-size distribution as a function of the strain in the submonolayer growth regime. Our island dynamics model is coupled to an elastic model that is based on atomistic harmonic interactions. The elastic equations are solved self-consistently at every time step during the simulation for the entire system. This is possible because the numerical time steps in the island dynamics model that is based on the level set technique are significantly larger than the time step of a typical atomistic event such as adatom diffusion and detachment while we still retain all the relevant physics that are associated with adatom diffusion and detachment.

DOI: 10.1103/PhysRevB.80.155309 PACS number(s): 68.55.−a

I. INTRODUCTION

Highly ordered and uniformly sized nanoscale patterns are of increasing relevance in many technological applications and have therefore been the focus of many recent studies. Application can range from storage devices[1] and catalysts[2] for metallic systems to so-called semiconductor quantum dots (QDs) for next generation optoelectronic devices.[3] A well-established fabrication process for such nanopatterns is to grow them via molecular-beam epitaxy. Optimal control in the synthesis of such nanopatterns requires a fundamental understanding of the processes during their growth. In this study, we focus on the submonolayer growth regime for such structures.

For many of these systems there is strain. For example, typical semiconductor systems used for QDs such as Ge/Si and $In_xGa_{1-x}As/GaAs$ have a lattice mismatch that leads to 4% and up to 7% strain in the system, respectively. This strain facilitates the formation and self-organization of arrays of nanopatterns and QDs.[4,5] However, the exact effect of strain on the driving forces is still not completely understood. For example, is the formation of ordered nanopatterns ultimately a thermodynamic effect or does strain mainly influence the kinetics during growth? To answer such questions, we need models that faithfully include the effects of strain.

It is difficult to properly include strain in a full three-dimensional simulation of epitaxial growth for systems of reasonable (and meaningful) size. The reason is that solving the elastic equations is rather expensive. It is almost prohibitively expensive to solve the elastic equations at every time step in an atomistic growth simulation, such as a kinetic Monte Carlo (KMC) simulation, where a typical numerical time step is the inverse of the diffusion constant and is often $O(10^{-6}$ s) (or smaller). We note that recent progress has made it possible to do such KMC simulations[6–8] but the system sizes studied are rather small and at present do barely allow any statistical analysis. We also note previous continuum-type work that studied the effect of strain on the coarsening dynamics of a two-dimensional array of islands.[9]

One way out of this dilemma is to not solve the elastic equations globally at every time step but to only solve them after a certain number of time steps and/or to solve them only locally (wherever the last event took place). A global update is then done periodically[10] and the frequency of this global update has to be tested carefully. Some insight can also be gained by focusing on two-dimensional models, where it is a lot faster to solve the elastic equations[11,12] or to study continuum-type models[13–15] that typically stress thermodynamic arguments but do not include the detailed kinetics. An alternative approach that we will describe below is to build a model where the numerical time step is significantly larger but where the model still properly accounts for the relevant atomistic events. In this approach one also has to make sure that the results are independent of the numerical time step. We also note a number of models where the main effect of strain is effectively accounted for by assuming an island size and/or height-dependent detachment[16,17] or where strain affects diffusion via a simple $1/r^3$ repulsion.[18]

In this paper, we present an island dynamics model that employs the level set technique[19–21] for the strain-driven regularization of islands during heteroepitaxy. A virtue and feature of this method is that we can solve the elastic equations for the entire system at every time step during the simulation. This is possible because a typical numerical time step is $O(10^{-2}-10^{-3}$ s), which is orders of magnitude larger than the time scale of microscopic events such as diffusion. Nevertheless, all the atomistic processes are included within this method. We show that strain leads to a regularization of island sizes in the submonolayer growth regime, as is evident from the narrowing and sharpening of the island-size distribution (ISD).

II. OUR MODEL

In our model for epitaxial growth, islands are described by a level set function and the growth of the islands is described by the time evolution of the level set function.[19–21] The velocity of the island boundaries is then obtained from

 ©2009 The American Physical Society

solving the following diffusion equation for the adatom concentration $\rho(\mathbf{x},t)$:

$$\frac{\partial \rho}{\partial t} = F + \nabla \cdot (\mathbf{D} \nabla \rho) - 2\frac{dN}{dt} + \nabla \cdot \left[\frac{\rho}{k_B T} \mathbf{D}(\nabla E_{\rm ad}) \right]. \quad (1)$$

In Eq. (1), $\mathbf{D}$ is a diffusion tensor where the diagonal entries are $D^{(i)}(\mathbf{x})$ and $D^{(j)}(\mathbf{x})$. F is the deposition flux, dN/dt is the nucleation rate, and the last term is the thermodynamic drift, where k_B is the Boltzmann constant and T is the temperature. The nucleation rate is given by

$$dN/dt = \sigma_1 \langle \{[D^{(i)}(\mathbf{x}) + D^{(j)}(\mathbf{x})]/2\} \rho^2(\mathbf{x}) \rangle. \quad (2)$$

where σ_1 is a capture number (that is, of order unity[22,23]) and the average $\langle \cdot \rangle$ is taken over all lattice sites.

Stochastic elements are required to properly describe island nucleation and the thermal dissociation of small islands. In particular, the rate of nucleation is deterministic, as described by Eq. (2), but the spatial position of a newly nucleated island is chosen with the probability that is weighted by the local value of $\rho^2(\mathbf{x})$.[24] Similarly, island breakup is correlated with the local detachment rate $D_{\rm det}(\mathbf{x})$ and the probability to shrink below the size of a dimer.[19] Once an island has been broken up, we assume fast diffusion and for simplicity distribute the mass of the island uniformly over the entire lattice. The detachment rate used in our model is an effective detachment rate, that is, the average rate for an atom to detach from a boundary (regardless of coordination) *and* to subsequently diffuse out of the capture area of the islands. In other words, we allow for detachment but do not resolve every detachment and subsequent reattachment event. This effective detachment rate has been carefully tested and we refer the reader to Ref. 19. We also note that a coordination- (or island shape) dependent detachment rate could be incorporated but this would not affect the basic message of this paper.

For the solution of Eq. (1) we enforce the boundary condition

$$\rho_0(\mathbf{x}) = \rho_{\rm eq}[D_{\rm edge}(\mathbf{x}), D_{\rm det}(\mathbf{x}), \mathbf{x}], \quad (3)$$

where $D_{\rm edge}(\mathbf{x})$ is the spatially varying microscopic rate for edge diffusion.[25] We highlight, in particular, the dependence on $D_{\rm det}$: the higher the detachment rate of adatoms, the higher the value of ρ_0 at the island boundary.

Our elastic model is essentially an atomistic cubic model that includes harmonic nearest- and next-nearest-neighbor terms. We assume that nearest-neighbor springs are twice as strong as next-nearest-neighbor springs. We define a discrete profile from the level set function as follows:

$$h_{ij} = [\phi_{ij}],$$

where $[\cdot]$ denotes the integer part. At each grid point in the film there is a displacement field defined, $\mathbf{u}_{ijk}$. These displacements satisfy a large linear system that is given in Ref. 7. The total elastic energy can be written as

$$W = \frac{\lambda}{2} \sum_{\text{all atoms}} E_{\rm strain}(\mathbf{x}),$$

where $E_{\rm strain}(\mathbf{x})$ is the energy contained in all the springs connected to the atom located at position $\mathbf{x}$. The expression we use is an extension to three dimensions from the two-dimensional formula found in Ref. 26. The scale factor λ is chosen so that the strain energy per atom in a fully strained system is approx. 0.04 eV for a system with 1% misfit and 0.6 eV for a system with 4% misfit. These numbers are plausible for typical semiconductor systems but we note that all our results can easily be rescaled (i.e., when we quote below results for 1% and 5% misfit, this might be a slightly different misfit for a particular system). Moreover, the main purpose of this paper is to report a qualitative trend, as strain increases.

For each time step we demand that the film is in mechanical equilibrium. This entails solving a large linear system. The substrate is semi-infinite with the same elastic properties as the film. It is fully relaxed each time the elastic field is updated. We use an artificial boundary condition to efficiently include the relaxation of the semi-infinite substrate. This boundary condition is carefully explained in Ref. 7. The resulting system is solved with a multigrid-Fourier method. For details see Ref. 27.

In principle, all of the microscopic parameters $D^{(i)}(\mathbf{x})$, $D^{(j)}(\mathbf{x})$, $D_{\rm det}(\mathbf{x})$, and $D_{\rm edge}(\mathbf{x})$ are affected by strain. We found that the effect on $D_{\rm edge}(\mathbf{x})$ is essentially irrelevant (since islands are always rather compact within the model) and leave $D_{\rm edge}(\mathbf{x})=0$. We choose $D^{(i)}(\mathbf{x})$ and $D^{(j)}(\mathbf{x})$ such that their value is 10^6 s^{-1} without strain. The growth temperature and deposition flux are chosen as $T=700$ K and $F=1.0$ ML/s^{-1}. We then parameterize the strain dependence according to density-functional theory (DFT) results for a typical semiconductor system[28,29] but also found that the effect of strain-dependent diffusion parameters is almost irrelevant for the strain-driven regularization of the ISD discussed below. This is different from our work on stacked quantum dots,[29] where we found that the strain-driven variation in $D^{(i)}(\mathbf{x})$ and $D^{(j)}(\mathbf{x})$ is crucial for the *placement* of islands.

The main effect of strain is the dependence of $D_{\rm det}$ on it. We are not aware of any DFT results or other systematic study of the dependence of $D_{\rm det}$ on strain. But we believe that it is quite plausible that detachment is enhanced upon both compressive and tensile strain, and preliminary (unpublished) DFT calculations by us support this assumption. More precisely, we assume that detachment is enhanced according to

$$D_{\rm det}(\mathbf{x}) = D^0_{\rm det}(\mathbf{x}) \exp[E_{\rm strain}(\mathbf{x})/k_B T], \quad (4)$$

where $D^0_{\rm det}(\mathbf{x})$ is the detachment rate for the unstrained system. $D^0_{\rm det}(\mathbf{x})$ was chosen to be 30 s^{-1} but we note that our interpretation of $D_{\rm det}$ is different than a detachment rate in an atomistic simulation (such as a KMC simulation) and that in fact the value 30 s^{-1} corresponds to a much higher atomistic detachment rate. The reason is that our $D_{\rm det}$ is an effective

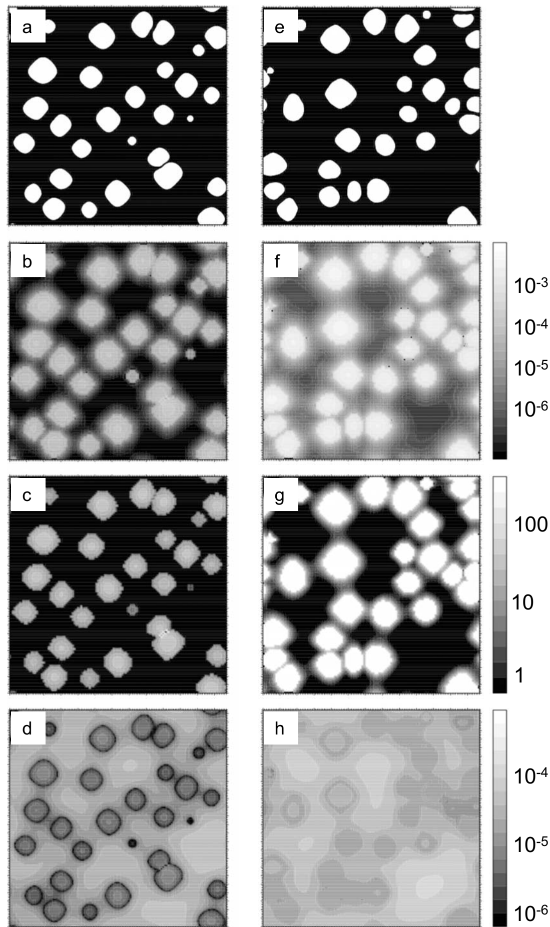

FIG. 1. The effect of strain in our model. We show results for 1% strain (left column) and 5% strain (right column). Shown are typical morphologies after a coverage of 20% (a) and (e), the corresponding elastic energy on the surface (b) and (f), the resulting detachment rates (c) and (g), and adatom concentrations (d) and (h). The units of the elastic energy are in terms of the spring constants that are O(1). The units of the adatoms concentration are adatoms per lattice sites. The units of the detachment rate are the number of detachment events per second. Note that the detachment rates are effective numbers that are smaller than in an atomistic (KMC) simulation; we only consider detachment events where the adatoms do not reattach to the island. The results shown were obtained for systems of size 180×180 (in units of atomic lattice constants).

parameter that combines detachment from an island boundary and escape from the capture zone of the island under consideration.[19] It would therefore be difficult to have a direct numerical comparison with such an atomistic simulation.

III. RESULTS

The parameter D_{det} describes the breakup of small islands (dimers) and the detachment of atoms from (larger) islands. The effect of strain in our model on the latter is illustrated in more detail in Fig. 1. We show a typical island morphology [(a) and (e)], the resulting strain energy [(b) and (f)] and its effect on the detachment rate [(c) and (g)], and boundary value $\rho_0(\mathbf{x})$ [(d) and (g)] for a system with small strain (left) and high strain (right). It is evident that the strain energy in the middle of the islands as well as around the island edges is significantly higher for the system with larger strain (f). As a result, the detachment rate as calculated according to Eq. (4) is significantly enhanced (g), which leads to a higher value for ρ_0 (h). We note that D_{det} and ρ_0 are defined for the entire system [as can be seen in Figs. 1(c), 1(d), 1(g), and 1(h)] but they only have physical meaning around the island boundaries. All results shown were obtained for systems of lateral size 180 (in dimensionless units), with a numerical resolution of 256 grid points laterally. We have carefully tested that the results are not influenced by the system size.

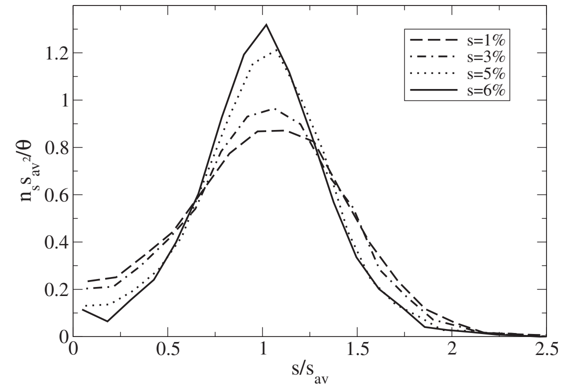

FIG. 2. The scaled island-size distribution after the deposition of 20% of a monolayer for different values of strain. n_s is the number of islands of size s, s_{av} is the average island size, and Θ is the coverage.

The increased value for ρ_0 at the island boundary implies that the gradients of ρ are less steep at the boundaries of islands with higher strain so that islands with more strain grow slower than less strained islands. Since smaller islands are less strained than larger islands, strain slows down growth of the larger islands more than growth of the smaller islands, which contributes to the regularization of the island sizes. This can be seen by comparing Figs. 1(a) and 1(e), where it appears that there are more really small islands in (a) and also a few rather large ones.

An additional and even more important contribution to the regularization of the islands is the fact that for systems with large strain, small islands (i.e., dimers) are less stable against breakup because even for islands as small as a dimer, strain enhances the detachment rate (which is the same as the breakup rate for a dimer). It is well known that enhanced breakup for dimers also leads to a sharper ISD. The reason is that small islands that have nucleated in an unfavorable spot (close to existing, bigger islands) have an enhanced chance to breakup and to subsequently renucleate in a more favorable spot. If the islands are located further apart from each other, they compete less for additional adatoms and are also less strained. Therefore, they can grow to islands with a more regular ISD. In Fig. 2 we show the scaled ISD after the deposition of 20% of a monolayer, as a function of strain. The scaled ISD for the system with more strain is clearly narrower and sharper, which is equivalent to the statement that the ISD is more regular.

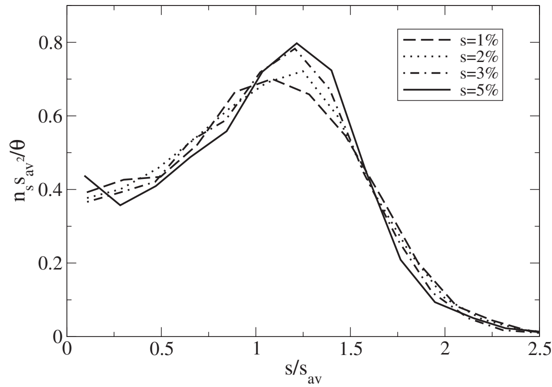

FIG. 3. The scaled island-size distribution with suppressed dimer breakup, after the deposition of 20% of a monolayer for different values of strain. n_s is the number of islands of size s, s_{av} is the average island size, and Θ is the coverage.

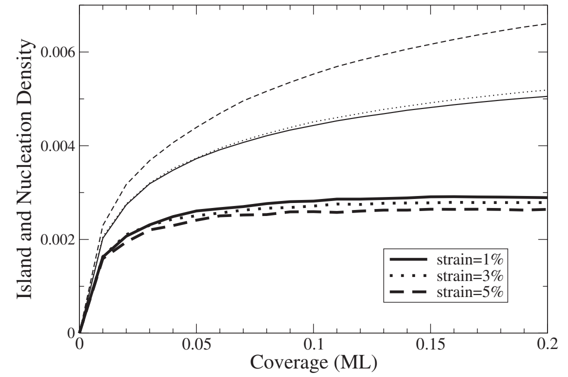

FIG. 4. Time evolution of the island densities (thick lines) and nucleation densities (thin lines) for different values of strain.

IV. DISCUSSION

In this section, we compare our results with previous theoretical and experimental works. The most relevant experimental studies are Refs. 30 and 31, which show the ISD in the submonolayer regime for InAs on GaAs(001), a system with 7% misfit. In addition to the ISD for the overall island size, both studies also show the ISD with respect to the lateral sizes along the [110] and [$\bar{1}$10] directions. In both studies the resulting ISD for the overall size and the ISD along the [$\bar{1}$10] resemble each other and the authors suggest that it is similar to the ISD for homoepitaxy. Close inspection and comparison to both experimental[32] and computational[33] studies of the ISD as a function of reversibility (or temperature) indicate, however, that the ISDs shown in Refs. 30 and 31 agree best with the ISD for a system with some reversibility. Whether this reversibility is an effect of the experimental temperature or an effect of strain is not necessarily clear, even though the authors of Refs. 30 and 31 suggest that strain does not play a major role.

However, it is evident in Refs. 30 and 31 that along the [110] direction the ISD is clearly influenced by strain. After the average island size reaches a certain value it does not grow any more with increasing coverage. In other words, the lateral size of the islands along the [110] direction is quenched by strain. This scenario (quenched island size along the [110] direction) agrees well with the results obtained in our model described above, where we describe how strain slows down growth of islands as they get bigger (and smaller ones "catch up"). We note that both of the experimental papers do not study the effect of increasing strain, as the misfit for InAs on GaAs is fixed at 7%. It is therefore difficult to say with certainty whether our results are or are not in agreement with the experiment. We also note in passing the work of Leonard *et al.*[34] for multilayer growth of $In_xGa_{1-x}As$ on GaAs(100). In this study, the authors varied the composition parameter x (and thus the misfit). The resulting ISDs for the multilayer dots appear to sharpen slightly with increasing strain. But since this is the multilayer regime, these results are not directly comparable to our results.

Our results that the ISD sharpens with increasing strain agree well with older KMC results,[16] where the effect of strain was approximated by a size-dependent detachment rate. But our results differ from simulation by Nandipati and Amar,[18] and also more recent KMC simulations by Aqua and Frisch.[8] The explanation for this is the following: Nandipati and Amar[18] presented results for the effects of strain on the ISD for irreversible growth. But as we will discuss below, the main contribution to the sharpening of the ISD is the enhanced breakup of small islands upon increasing strain. Aqua and Frisch[8] do have a model that includes breakup of small islands. But they choose parameters such that the detachment rate is only increased by a factor of ~2, which is not enough to see an effect on the ISD. In comparison, in our work typical detachment rates are enhanced by a factor of ~2 for 1% misfit but by up to a factor of ~500 for 5% misfit.

The importance of the strain enhanced breakup of small islands on the sharpening of the ISD is illustrated in Fig. 3. Here, we present results with the same parameters as above but do artificially suppress breakup. Growth of bigger islands is still slowed down with increasing strain (so that small islands can catch up). It is evident that the ISD sharpens very little, which confirms that the enhanced breakup (and renucleation) of small islands is the main driving force for the sharpening of the ISD.

We also want to discuss the evolution of the island density (or average island size) as a function of strain. In Figs. 1(a) and 1(e) it appears that the island density is essentially unchanged with strain, which is in contrast to the expectation that more strain leads to more (and smaller) islands. The reason is the following: while thermodynamic arguments favor an increased island density (smaller islands) upon increasing strain, there is also an enhanced breakup of islands. So there is a complicated interplay between these two opposing mechanisms. In Fig. 4 we show that the island densities are almost unchanged as strain increases (solid lines) while the number of nucleation events increases more than threefold (thin lines). But as explained above, more nucleation does not necessarily lead to more islands on the surface. In fact, it has been known for a long time that without strain, enhanced breakup leads to fewer and larger islands.[33]

V. SUMMARY

The results presented in this communication illustrate that an island dynamics model that is coupled to the level set

method is well suited to model epitaxial growth of strained systems. We have focused in this paper on the submonolayer growth regime. As a next step, we will show that this method can also be extended to model multilayer growth and the formation of full QDs. But some challenges still remain for this extension. In particular, the boundary condition (3) needs to be changed to the more general mixed Robin boundary condition $\partial\rho/\partial n+\alpha\rho=\beta$, to account for an additional step-edge barrier for interlayer mass transport, and its dependence on strain. This requires new numerical schemes to solve the diffusion Eq. (1) and is work that is currently in progress.

ACKNOWLEDGMENTS

This research was supported in part by the MARCO Center on Functional Engineered NanoArchitectonics (FENA) and by the NSF through Grants No. DMS 0509124, No. DMS 0553487, No. DMS 0810113, No. DMS-0402276, and No. DMS-0439872.

[1] S. Sun, C. B. Murray, D. Weller, L. Folks, and A. Moser, Science **287**, 1989 (2000).
[2] M. Valden, X. Lai, and D. W. Goodman, Science **281**, 1647 (1998).
[3] J. Stangl, V. Holy, and G. Bauer, Rev. Mod. Phys. **76**, 725 (2004).
[4] D. J. Eaglesham and M. Cerullo, Phys. Rev. Lett. **64**, 1943 (1990).
[5] Y.-W. Mo, D. E. Savage, B. S. Swartzentruber, and M. G. Lagally, Phys. Rev. Lett. **65**, 1020 (1990).
[6] M. T. Lung, C.-H. Lam, and L. M. Sander, Phys. Rev. Lett. **95**, 086102 (2005).
[7] G. Russo and P. Smereka, J. Comput. Phys. **214**, 809 (2006).
[8] J.-N. Aqua and T. Frisch, Phys. Rev. B **78**, 121305(R) (2008).
[9] F. Liu, A. H. Li, and M. G. Lagally, Phys. Rev. Lett. **87**, 126103 (2001).
[10] B. G. Orr, D. Kessler, C. W. Snyder, and L. Sander, Europhys. Lett. **19**, 33 (1992).
[11] C.-H. Lam, C.-K. Lee, and L. M. Sander, Phys. Rev. Lett. **89**, 216102 (2002).
[12] F. Much and M. Biehl, Europhys. Lett. **63**, 14 (2003).
[13] J. Tersoff and R. M. Tromp, Phys. Rev. Lett. **70**, 2782 (1993).
[14] J. Tersoff, C. Teichert, and M. G. Lagally, Phys. Rev. Lett. **76**, 1675 (1996).
[15] C.-h. Chiu and C. T. Poh, Phys. Rev. B **71**, 045406 (2005).
[16] C. Ratsch, A. Zangwill, and P. Šmilauer, Surf. Sci. **314**, L937 (1994).
[17] C. Ratsch, P. Šmilauer, D. D. Vvedensky, and A. Zangwill, J. Phys. I **6**, 575 (1996).
[18] G. Nandipati and J. G. Amar, Phys. Rev. B **73**, 045409 (2006).
[19] M. Petersen, C. Ratsch, R. E. Caflisch, and A. Zangwill, Phys. Rev. E **64**, 061602 (2001).
[20] C. Ratsch, M. F. Gyure, R. E. Caflisch, F. Gibou, M. Petersen, M. Kang, J. Garcia, and D. D. Vvedensky, Phys. Rev. B **65**, 195403 (2002).
[21] S. Chen, M. Kang, B. Merriman, R. E. Caflisch, C. Ratsch, R. Fedkiw, M. F. Gyure, and S. Osher, J. Comput. Phys. **167**, 475 (2001).
[22] J. Venables, Philos. Mag. **27**, 697 (1973).
[23] G. S. Bales and D. C. Chrzan, Phys. Rev. B **50**, 6057 (1994).
[24] C. Ratsch, M. F. Gyure, S. Chen, M. Kang, and D. D. Vvedensky, Phys. Rev. B **61**, R10598 (2000).
[25] R. E. Caflisch, W. E, M. F. Gyure, B. Merriman, and C. Ratsch, Phys. Rev. E **59**, 6879 (1999).
[26] T. P. Schulze and P. Smereka, J. Mech. Phys. Solids **57**, 521 (2009).
[27] G. Russo and P. Smereka, Multiscale Model. Simul. **5**, 130 (2006).
[28] E. Penev, P. Kratzer, and M. Scheffler, Phys. Rev. B **64**, 085401 (2001).
[29] X. B. Niu, Y.-J. Lee, R. E. Caflisch, and C. Ratsch, Phys. Rev. Lett. **101**, 086103 (2008).
[30] V. Bressler-Hill, S. Varma, A. Lorke, B. Z. Nosho, P. M. Petroff, and W. H. Weinberg, Phys. Rev. Lett. **74**, 3209 (1995).
[31] G. R. Bell, T. J. Krzyzewski, P. B. Joyce, and T. S. Jones, Phys. Rev. B **61**, R10551 (2000).
[32] J. A. Stroscio and D. T. Pierce, Phys. Rev. B **49**, 8522 (1994).
[33] C. Ratsch, P. Šmilauer, A. Zangwill, and D. D. Vvedensky, Surf. Sci. **329**, L599 (1995).
[34] D. Leonard, M. Krishnamurthy, S. Fafard, J. L. Merz, and P. M. Petroff, J. Vac. Sci. Technol. B **12**, 1063 (1994).